IEEE Access
Multidisciplinary | Rapid Review | Open Access Journal

Received May 29, 2019, accepted July 9, 2019, date of publication July 24, 2019, date of current version August 7, 2019.

Digital Object Identifier 10.1109/ACCESS.2019.2930102

Extrapolation-RELAX Estimator Based on Spectrum Partitioning for DOA Estimation of FMCW Radar

SANGDONG KIM, BONG-SEOK KIM, YOUNGSEOK JIN, AND JONGHUN LEE, (Senior Member, IEEE)

Advanced Radar Technology (ART) Laboratory, Convergence Research Center for Future Automotive Technology, Daegu Gyeongbuk Institute of Science and Technology, Daegu 42988, South Korea

Corresponding author: Jonghun Lee (jhlee@dgist.ac.kr)

This work was supported in part by the DGIST and in part by the DGIST Research and Development Program of the Ministry of Science, ICT and Future Planning, South Korea, under Grant 19-IT-01 and Grant 19-02-HRHR-03.

ABSTRACT This paper proposes an extrapolation-RELAX estimator based on spectrum partitioning (SP) for the direction of arrival (DOA) estimation of frequency-modulated continuous-wave (FMCW) radar. The FMCW radar employs fast Fourier transform (FFT)-based digital beamforming (DBF) for the DOA estimation owing to its low complexity and easy implementation. However, the DBF algorithm has a disadvantage of low angle resolution. To improve the angle resolution, super-resolution algorithms such as multiple signal classification (MUSIC) and estimation of signal parameters via rotational invariance techniques (ESPRIT) are proposed. However, these algorithms require the high signal-to-noise ratio (SNR) to meet the required performance. To overcome this drawback of super-resolution algorithms, the SP-based extrapolation method has been proposed. However, this algorithm still has the problem that the resolution performance degrades owing to the insufficient number of actual antenna arrays. To solve this problem, we propose the SP-based extrapolation-RELAX algorithm for DOA estimation of FMCW radar. Through extrapolation, the proposed structure solves the problem of insufficient number of arrays, resulting in high reliability of SP results. When the extrapolation algorithm is used to generate the input signal of the RELAX algorithm, the RELAX method improves the performance of the DOA estimation. To confirm the effectiveness of the proposed estimation, we compare the Monte Carlo simulation and root-mean-square error results of the proposed and conventional algorithms. To verify the performance of the proposed algorithm in practical conditions, experiments were performed using the FMCW radar module within a chamber and in an indoor environment.

INDEX TERMS Spectrum partitioning, extrapolation-RELAX, DBF, parameter estimator, FMCW radar.

I. INTRODUCTION

For a long time, several studies on radar sensors have been reported [1]–[4]. Radar sensors allow for the safe detection of targets because they are less sensitive to environmental conditions such as heavy rain, snow, and fog compared to other sensors such as cameras and LiDAR [5]. Due to these advantages, radar sensors have been employed across several applications. For example, radar sensors have been used for automotive applications such as adaptive cruise control, collision avoidance, and parking aid [3]. In addition, radar sensors have been employed in not only military applications such as detection of the tank and aircraft of enemy but also surveillance applications [6].

Among the radar sensors, Doppler radar systems have been widely used due to its advantages such as low cost and low complexity compared to other radar systems. Doppler radar can easily estimate the velocity of the target using a frequency change proportional to the speed of the moving target [2]. However, Doppler radar systems have shortcoming that it cannot detect the distance of the target.

Meanwhile, in recent years, the detection of target was focused by various radar systems such as ultra-wideband (UWB) and frequency-modulated continuous

The associate editor coordinating the review of this manuscript and approving it for publication was Yejun He.

wave (FMCW). UWB radars have been used for the target detection [7], [8], imaging in through-wall conditions [9] and positioning indoors [10], [11] because of its high range resolution and penetrability [8]. Conventional studies on UWB radars are considered to suppress various clutters, estimating parameters to analyze signal characteristics, and other related problems. To suppress clutter, the classic ensemble empirical mode decomposition (EEMD) technique was used in a previous study [12] to estimate target position by improving the signal-to-noise ratio (SNR) and removing clutter. However, most detection techniques for UWB radars are ineffective at obtaining accurate direction of arrival (DOA) because the two or more UWB radars are needed to estimate DOA.

Owing to this, FMCW radar, which can detect the distance and Doppler information, has been considered as an alternative [13], [14]. FMCW radars have been used for the detection of targets [2] and moving subjects [15] owing to its high resolution and low cost. In conventional FMCW radar systems, FFT-based algorithms with low complexity are used to extract multiple parameters such as distance, Doppler information, or angle in order to obtain portability and low cost. However, the resolution and accuracy of the FFT-based parameter estimator are considerably low [13], [14]. Especially, DOA estimation is a major problem while estimating accurate position for FMCW radar. In particular, an FFT-based DOA estimation method called digital beamforming (DBF) has been widely used. However, as FFT has a low resolution, super-resolution algorithms such as multiple signal classification (MUSIC) and estimation of signal parameters via rotational invariance techniques (ESPRIT) have been used for DOA estimation.

Recently, an extrapolation algorithm based on spectrum partitioning (SP) among super-resolution algorithms have been studied [16]. Extrapolation based on SP improves the resolution of parameters in order to estimate the coefficient of autoregressive (AR) model. The SP-based extrapolation method first divides the spectrum data into a plenty of sub-bands after transforming the received signal into a spectrum. To improve the performance of DOA, the SP-based extrapolation algorithm can be applied to DOA estimation. A large number of antenna arrays in the sub-band can be used to obtain accurately coefficients for the AR model. However, in the case of various applications for FMCW radar, the number of actual antenna arrays still has a limitation in that the resolution performance of SP-based extrapolation is insufficient.

In order to solve this problem of SP-based extrapolation, we propose SP-based extrapolation-RELAX algorithm for DOA estimation of FMCW radar. Through extrapolation, the proposed structure solves the problem of insufficient number of arrays, resulting in high reliability of SP results. When the extrapolation algorithm with the high reliability of SP results is used as the input signal of the RELAX algorithm, the RELAX method improves the performance of the DOA. To enhance the performance of RELAX, extrapolation is needed to increase the number of virtual antenna arrays. After the received signal is applied into SP, extrapolation is applied to each partition result of the SP to increase the number of virtual arrays because the extrapolation algorithm can overcome the disadvantages of the low-resolution DBF based on FFT for DOA information. Subsequently, using characteristics that the spectrum output of the extrapolation includes magnitude and phase value while other super-resolution algorithms have only pseudo-magnitude information, the RELAX algorithm is applied to the results of the extrapolation with the SP method. Thus, the proposed structure is better than the resolution of each extrapolation and RELAX algorithm.

The remainder of this paper is organized as follows. Section II provides a brief review of the signal model for the distance, Doppler information, and angle of the FMCW radar. Section III presents the proposed extrapolation-RELAX estimator based on spectrum partitioning for DOA estimation of FMCW radar. This section also analyzes the complexity of each algorithm. Section IV shows the simulations for various environments. Experimental results are described in Section V. Finally, conclusions are provided in Section VI.

II. SIGNAL MODEL

This section shows the system models of the FMCW radar. The purpose of the FMCW radar is to estimate parameters such as distance, Doppler information, and angle of targets. Especially, the Doppler signal is obtained from the phase data of the reflected FMCW signal. The architecture of the FMCW radar is shown in Fig. 1. The transmitted (TX) signal is generated and transmitted, and then the reflected signal is obtained at the received (RX) part. The reflected signals are transformed into a linear combination of sinusoidal signals, the so-called beat signal, as shown in Fig. 1 [2]. The sinusoidal signal has a frequency proportional to time delay between the FMCW radar and the target.

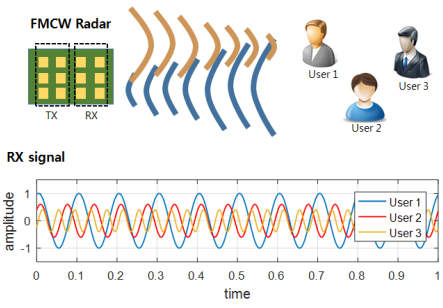

FIGURE 1. FMCW radar architecture.

The FMCW TX signal $s_{\mathrm{TX}}(t)$ as shown in Fig. 2 (a) [2] is represented by

$$s_{\mathrm{TX}}(t) = \sum_{l=0}^{L-1} s_0(t - lT_F) \tag{1}$$

where L indicates the number of FMCW chirp signals, T_F denotes the total duration of chirp symbol and idle period, i.e., $T_F = T + T_i$, T indicates the duration of chirp symbol,

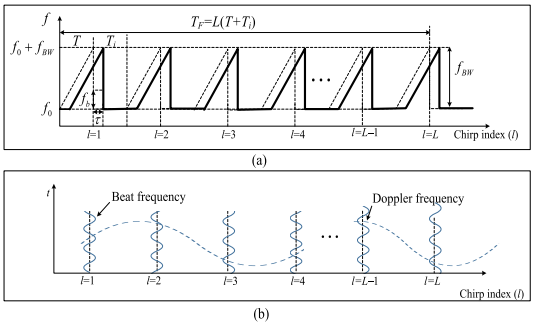

FIGURE 2. Waveforms of the FMCW radar: (a) TX signal (dashed line) and RX signal (solid line); (b) beat signal [2].

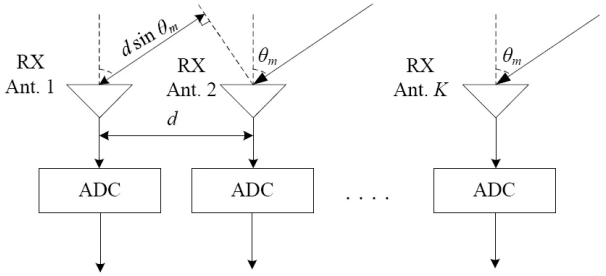

FIGURE 3. DOA architecture.

and T_i represents the duration of the idle period. The FMCW chirp symbol $s_0(t)$ is expressed as

$$s_0(t) = \begin{cases} \exp\left(j(2\pi f_0 t + \dfrac{\mu t^2}{2})\right), & \text{for } 0 \le t < T \\ 0, & \text{elsewhere} \end{cases} \quad (2)$$

where f_0 denotes the initial frequency, $\mu = 2\pi f_{\mathrm{BW}}/T$ denotes the frequency slope of the FMCW chirp symbol depending on time, and f_{BW} represents the bandwidth of the FMCW signal.

For Doppler estimation of M targets as shown in Fig. 2, f_D is defined as the Doppler frequency. The Doppler results derived with c as the speed of wave and v as the target velocity yield the shifted frequency f_{r} as a function of the initial frequency f_0 as

$$f_{\mathrm{r}} = f_0\left(\frac{1+v/c}{1-v/c}\right) \quad (3)$$

where the Doppler frequency $f_D = f_{\mathrm{r}} - f_{\mathrm{c}} = 2\,vf_0/\mathrm{c}$. The Doppler frequency-based received signal in the first array is composed of

$$y_{1,l}(t) = \sum_{m=0}^{M-1}\left[\tilde{a}_m s_{\mathrm{TX}}(t-\tau_m)\exp\left(j2\pi f_m^D l T_F\right)\right] + \omega(t) \quad (4)$$

where $\tilde{a}_m$ is the m-th target's complex amplitude, f_m^D is Doppler frequency of the m-th target, and $\omega(t)$ defines the additive white Gaussian noise (AWGN) signal.

As a uniform linear array (ULA) comprising K antenna elements is considered in Fig. 3, the reflected signal from the m-th target is received with the time delay τ_m. The l-th received chirp symbol $y_l(t)$ in the k-th antenna array is shown in (5), as shown at the bottom of this page, where λ is the carrier frequency's wavelength, d denotes the distance from k-th to $(k+1)$-th antenna element, and θ_m defines the DOA of m-th target. In RX parts, the de-chirping method is used to reduce the complexity of the FMCW radar. The de-chirping method defines the conjugation multiplication technique of the FMCW TX signals $s_{\mathrm{TX}}^*(t)$ and the received FMCW signals of the l-th symbol and the k-th antenna array $y_{k,l}(t)$, and the beat signal at the l-th chirp symbol and k-th antenna array $p_{k,l}(t)$ is expressed as

$$p_{k,l}(t) = y_{k,l}(t)s_{\mathrm{TX}}^*(t). \quad (6)$$

By substituting (5) into (6), the dechirped FMCW signal $p_{k,l}(t)$ is expressed in the form of a product of sinusoidal waveforms as shown in (7), as shown at the top of the next page.

When the Nyquist sampling frequency is determined to be $f_s = 1/T_s$, the discrete signal $p_{k,l}[n]$ of $p_{k,l}(t)$, for $n = 0, 1, \ldots N-1$, through an analog-to-digital converter (ADC) can be described as (8), as shown at the top of the next page. The data from (8) can be arranged into a vector $\boldsymbol{p}_{k,l} = \left[p_{k,l}[0], p_{k,l}[1], \ldots, p_{k,l}[N-1]\right]^{\mathrm{T}}$ and $\boldsymbol{p}_{k,l}$ is represented by the range, velocity, and DOA terms, respectively, as follows:

$$\boldsymbol{p}_{k,l} = \boldsymbol{\alpha}\boldsymbol{v}_l\boldsymbol{d}_k\boldsymbol{B} + \boldsymbol{\omega} \quad (9)$$

where $\boldsymbol{\alpha}$ and $\boldsymbol{\omega}$ are the vector composed of amplitude and noise terms, respectively, i.e., $\boldsymbol{\alpha} = [a_0, a_1, \ldots, a_{N-1}]^{\mathrm{T}}$ and $\boldsymbol{\omega} = [\omega_0, \omega_1, \ldots, \omega_{N-1}]^{\mathrm{T}}$, $\boldsymbol{B}$ is the vector of the range term, i.e., $\boldsymbol{B} = [B(\tau_0), B(\tau_1), \ldots, B(\tau_M)]$ where $B(\tau_m)$ is FMCW beat signal due to delay τ_m, i.e., $B(\tau_m) = \exp(j2\pi\mu\tau_m T_s n)$, $\boldsymbol{v}_l$ is the vector of the velocity term, i.e., $\boldsymbol{v}_l$ is expressed as

$$\boldsymbol{v}_l = \mathrm{diag}\left[v_l(0), v_l(1), \ldots, v_l(M-1)\right] \quad (10)$$

where diag$(\cdot)$ denotes a matrix operator with the elements of vector on the main diagonal wherein the off-diagonal elements are all zero and the m-th element of $\boldsymbol{v}_l$, $v_l(m)$ is expressed as

$$v_l(m) = \exp\left(j2\pi f_m^D l T_F\right). \quad (11)$$

In (9), $\boldsymbol{d}_k$ denotes the vector of DOA term, i.e., $\boldsymbol{d}_k = \mathrm{diag}\left[d_k(0), d_k(1), \ldots, d_k(M-1)\right]$ where the m-th element of

$$y_{k,l}(t) = \sum_{m=0}^{M-1}\left[\tilde{a}_m s_{\mathrm{tx}}(t-\tau_m)\exp\left(j2\pi f_m^D l T_F\right)\exp\left(\frac{j2\pi}{\lambda}dk\sin\theta_m\right)\right] + \omega(t) \quad (5)$$

$$p_{k,l}(t) = \sum_{m=0}^{M-1}\left[\tilde{a}_m \exp\left(j\left(2\pi\mu\tau_m t + \omega_s\tau_m - \mu\tau_m^2/2\right)\right)\exp\left(j2\pi f_m^D l T_F\right)\exp\left(\frac{j2\pi}{\lambda}dk\sin\theta_m\right)\right] + \omega(t)$$

$$= \sum_{m=0}^{M-1}\left[\underbrace{\tilde{a}_m \exp\left(\omega_s\tau_m - \mu\tau_m^2/2\right)}_{\equiv a_m}\exp\left(j2\pi\mu\tau_m t\right)\exp\left(j2\pi f_m^D l T_F\right)\exp\left(\frac{j2\pi}{\lambda}dk\sin\theta_m\right)\right] + \omega(t)$$

$$= \sum_{m=0}^{M-1}\left[a_m \underbrace{\exp\left(j2\pi\mu\tau_m t\right)}_{\text{distance}}\underbrace{\exp\left(j2\pi f_m^D l T_F\right)}_{\text{Doppler}}\underbrace{\exp\left(\frac{j2\pi}{\lambda}dk\sin\theta_m\right)}_{\text{angle}}\right] + \omega(t) \tag{7}$$

$$p_{k,l}[n] = \sum_{m=0}^{M-1}\left[a_m \exp\left(j2\pi\mu\tau_m T_s n\right)\exp\left(j2\pi f_m^D l T_F\right)\exp\left(\frac{j2\pi}{\lambda}dk\sin\theta_m\right)\right] + \omega[n] \tag{8}$$

$\boldsymbol{d}_k$, $d_k(m)$ is expressed as

$$d_k(m) = \exp\left(\frac{j2\pi}{\lambda}dk\sin\theta_m\right). \tag{12}$$

III. PROPOSED EXTRAPOLATION-RELAX ESTIMATOR BASED ON SPECTRUM PARTITIONING FOR DOA ESTIMATION OF FMCW RADAR

This section proposes an extrapolation-RELAX estimator based on SP for DOA estimation of the FMCW radar. This algorithm aims to enhance DOA resolution compared with the conventional estimator. As the number of antenna arrays is insufficient owing to their high cost and DBF is used by FFT algorithm [3], the conventional FMCW's DOA resolution is low. As this paper focuses on DOA detection, Doppler information is omitted.

A. FFT FOR DISTANCE INFORMATION

The proposed method first estimates the distance information of multiple targets from the received beat signal [3]. After the received signal is processed by 1D-FFT, the distance index of various targets is extracted through threshold detection, and the FFT magnitude component corresponding to the distance index is obtained. For threshold detection, the fixed value is used, and the maximum peak value among the extracted data is selected. As shown in Fig, 2, first, the time delay term to estimate the distance of the target and the Doppler term to estimate the parameter information of the target are determined using 2D-FFT [13]. For distance estimation, 1D-FFT [3] is performed on the received chirp signals with the l-th chirp index and k-th antenna array obtained. The 1D-FFT results $\boldsymbol{P}_{k,l} = [P_{k,l}[0], P_{k,l}[1], \ldots, P_{k,l}[N-1]]^{\mathrm{T}}$ at the k-th antenna array, l-th chirp symbol, and s-th frequency index-based distance information FFT output are expressed as

$$\boldsymbol{P}_{k,l} = \boldsymbol{W}_N \boldsymbol{p}_{k,l} \tag{13}$$

where $\boldsymbol{W}_N$ is the DFT matrix composed of N column vectors with N by 1 size, i.e., $\boldsymbol{W}_N = [W_0, W_1, \ldots, W_{N-1}]$ and the u-th column vector is denoted by W_u and is expressed as

$$W_u = \left[1, \exp\left(-j\frac{2\pi u}{N}\right), \ldots, \exp\left(-j\frac{2\pi u(N-1)}{N}\right)\right]^{\mathrm{T}}. \tag{14}$$

To detect the distance information of the target, this study uses the 1D-FFT results of multiple chirp using $\boldsymbol{P}_{k,1}, \boldsymbol{P}_{k,2,\ldots,}\boldsymbol{P}_{k,L}$. The differentiator using multiple chirp sample-by-sample can be obtained through the following formula

$$\boldsymbol{P}_{k,l}^{\mathrm{diff}} = \boldsymbol{P}_{k,l+1} - \boldsymbol{P}_{k,l} \tag{15}$$

After the differentiator of 1D-FFT is accomplished, the peaks among the distance spectrum $\boldsymbol{I} = [I_1, I_2, \ldots, I_M]$ are detected and the peak index indicates the distance results of targets. Using the peak value of differentiator using distance 1D-FFT, super-resolution DOA results are obtained, which are discussed in Section III B.

B. PROPOSED METHOD FOR ANGLE INFORMATION

After the target's distance information is detected by the differentiator of 1D-FFT from Section III A, we need to obtain the DOA information from the magnitude and phase information of detected 1D-FFT results. To obtain the super-resolution DOA results, we need to transform the extracted 1D-FFT results into the frequency spectrum. At the l-th chirp symbol, we define the input of DOA for the m-th target $\boldsymbol{P}_{m,l}^{\mathrm{array}} = \left[P_{0,l}[I_m], P_{1,l}[I_m], \ldots, P_{K-1,l}[I_m]\right]^{\mathrm{T}}$ and the DOA FFT results $\boldsymbol{R}_{m,l} = \left[R_{m,l}[0], R_{m,l}[1], \ldots, R_{m,l}[K-1]\right]^{\mathrm{T}}$ as a frequency transform such that

$$\boldsymbol{R}_{m,l} = \boldsymbol{W}_K \boldsymbol{P}_{m,l}^{\mathrm{array}}. \tag{16}$$

We can describe a spectral partition matrix S_Z for the z-th sub-band $z = 0, 1, \ldots, Z-1$ as

$$\boldsymbol{S}_z \equiv \mathrm{diag}(s_0^z, s_1^z, \ldots, s_{K-1}^z) \tag{17}$$

where the diagonal element is given by

$$s_i^z = \begin{cases} 1 & i \in I_z \\ 0 & \text{otherwise} \end{cases} \tag{18}$$

Here, I_z is a parameter set of indexes defined as

$$I_z \equiv \left[i_{z,j}\right]_{j=0}^{A-1} \quad \text{with } i_{z,j} = ((z-1)A + j) \tag{19}$$

where A is the size of sub-bands, i.e., $A = K/Z$, and integer values. The spectral partitioning results in the z-th sub-band can then be expressed as

$$\boldsymbol{R}_{m,l}^{\mathrm{s}} = \boldsymbol{S}_z \boldsymbol{R}_{m,l}. \tag{20}$$

After spectral partitioning, an inverse FFT can be applied to $\boldsymbol{R}_{m,l}^{\mathrm{s}}$ to obtain a data sequence for the signal within the z-th sub-band such as

$$\boldsymbol{P}_{m,l}^{\mathrm{SA}} = \boldsymbol{W}_{\mathrm{K}}^{-1} \boldsymbol{R}_{m,l}^{\mathrm{s}} \tag{21}$$

where $\boldsymbol{P}_{m,l}^{\mathrm{SA}} = \left[P_{m,l}^{\mathrm{SA}}[0], P_{m,l}^{\mathrm{SA}}[1], \ldots, P_{m,l}^{\mathrm{SA}}[K-1]\right]^{\mathrm{T}}$.

To perform DOA extrapolation using the inverse FFT signal $\boldsymbol{P}_{m,l}^{\mathrm{SA}}$, AR parameters are estimated from each chirp signal, and linear prediction is performed with the estimated parameters. The model-based techniques depend on modeling the data sequence as the output of a linear system of a rational system form such as

$$H(\theta) = \frac{B(\theta)}{A(\theta)} = \frac{\sum_{k=0}^{q} b(k) \exp\left(-j\pi k \sin\theta\right)}{1 + \sum_{k=1}^{p} a(k) \exp\left(-j\pi k \sin\theta\right)}. \tag{22}$$

This mathematical model that represents the given data sequence by the pole–zero linear model is called an autoregressive-moving average (ARMA) model. This model comprises the ARMA model, AR model, and moving-average (MA) model with the p and q values. Among these three linear models, the AR model with $q = 0$ is the most widely used approach because the AR model results can represent sharp peaks [17].

Using the AR model, the signal in the l-th chirp symbol and m-th target can be modeled as

$$P_{m,l}^{\mathrm{SA}}[0] = -\sum_{k=1}^{p} a[k] P_{m,l}^{\mathrm{SA}}[k] + \varepsilon[n] \tag{23}$$

In this case, the power spectrum $P_x(z)$ of a p-th order AR process is defined as follows:

$$\hat{P}(\theta) = \frac{|b[0]|^2}{\left|1 + \sum_{k=1}^{p} a[k] \exp\left(-j\pi k \sin\theta\right)\right|^2} \tag{24}$$

where $b(0)$ and $a(k)$ can be estimated from the data and the accuracy of spectrum estimation, $\hat{P}(\theta)$ will depend on how accurately the model parameters may be estimated, and $\varepsilon[n]$ indicates the modeling error, which is assumed to be random noise. As the AR spectrum estimation requires that an all-pole model be obtained for the process, a variety of techniques may be used to estimate the all pole parameter $a[k]$ [17]. However, once the all-pole parameters have been estimated, each method generates an estimate of the power spectrum in exactly the same manner. The typical method to estimate an AR parameter for estimating distance information is the covariance method [17]. To find the p-th order AR parameters $\hat{\boldsymbol{a}} = \left[\hat{a}(1), \hat{a}(2), \cdots, \hat{a}(p)\right]^{\mathrm{T}}$ the covariance method requires a set of linear equations such as

$$\begin{bmatrix} c_x(1,1) & c_x(2,1) & \cdots & c_x(p,1) \\ c_x(1,2) & c_x(2,2) & \cdots & c_x(p,2) \\ \vdots & \vdots & \ddots & \vdots \\ c_x(1,p) & c_x(2,p) & \cdots & c_x(p,p) \end{bmatrix} \begin{bmatrix} \hat{a}(1) \\ \hat{a}(2) \\ \vdots \\ \hat{a}(p) \end{bmatrix} = -\begin{bmatrix} c_x(1) \\ c_x(2) \\ \vdots \\ c_x(p) \end{bmatrix}. \tag{25}$$

The autocorrelation sequence $c_x(k,l)$ is defined as

$$c_x(a,b) = P_{m,l}^{\mathrm{SA}}[a] P_{m,l}^{\mathrm{SA}}[b]^* \tag{26}$$

For DOA spectrum estimation using the AR model, the order of the AR process p should be determined by the number of targets M. When the order p is smaller than the number of targets M, the results of the DOA spectrum will be smoothed and will have low resolution. When the order p is larger than the number of targets M, the results of the DOA spectrum will have spurious peaks. Another method of determining the model order p involves the use of the Akaike information criterion (AIC) and minimum description length (MDL) [18], [19]. The optimal modeling order can be selected by changing the model order until the values of the MDL or the AIC are minimized.

After the number of virtual arrays is increased to perform extrapolation, we can achieve the RELAX algorithm to enhance the DOA resolution. The extrapolated virtual array vector $\boldsymbol{P}_{m,l}^{\mathrm{VA}} = \left[P_{0,l}[I_m], P_{1,l}[I_m], \ldots, P_{K_E-1,l}[I_m]\right]^{\mathrm{T}}$ with a number of extrapolated arrays K_{E} and $P_{k,l}[I_m] = v_l(m) d_k(m)$ is fed into the input of the RELAX algorithm because the extrapolation results have the magnitude and phase information. For RELAX, first, we can set $\hat{a}_1 = 0$. $\hat{\theta}_1$ does not require the definition. After this process, we repeat first step $m = 1, 2, \ldots, M$ as follows

$$\hat{\theta}_m = \arg\max_{\theta} \frac{\left\|\boldsymbol{\alpha}^{\mathrm{H}}(\theta) \boldsymbol{P}_{m,l}^{\mathrm{VA}}\right\|^2}{\|\boldsymbol{\alpha}(\theta)\|^2} \tag{27}$$

$$\hat{a}_m = \frac{\boldsymbol{\alpha}^{\mathrm{H}}(\hat{\theta}_m) \boldsymbol{P}_{m,l}^{\mathrm{VA}}}{\left\|\boldsymbol{\alpha}(\hat{\theta}_m)\right\|^2} \tag{28}$$

where $\boldsymbol{\alpha}(\theta) = \left[1, \exp\left(\frac{j2\pi}{\lambda} d \sin\theta\right), \ldots, \exp\left(\frac{j2\pi}{\lambda} d K_E \sin\theta\right)\right]^{\mathrm{T}}$. The RELAX algorithm finishes when the maximum value of $\left\|\boldsymbol{\alpha}^{\mathrm{H}}(\theta) \boldsymbol{P}_{m,l}^{\mathrm{VA}}\right\|^2$ results is less than a pre-determined threshold.

C. SUMMARY OF THE PROPOSED ALGORITHM

The major steps of the proposed algorithm are as follows:

- **Step 1:** For distance estimation, the 1D-FFT is performed on the received chirp signals with the l-th chirp index and k-th antenna array obtained.
- **Step 2:** After the target's distance information is detected by the differentiator of the 1D-FFT, we obtained the DOA information from the magnitude and phase information of the detected 1D-FFT results.
- **Step 3:** In the case of the DOA, we obtained the results of the spectrum partitioning-extrapolation algorithm. Through extrapolation, the proposed structure solves the problem of insufficient number of arrays, resulting in high reliability of SP results.
- **Step 4:** After spectrum partitioning-extrapolation, we applied the RELAX algorithm to enhance the DOA resolution performance.
- **Step 5:** Finally, the DOA information with high resolution is obtained.

D. COMPLEXITY ANALYSIS

In this section, the complexities of the proposed algorithm and conventional ones such as the 2D-MUSIC and the 2D-FFT are determined and compared. The primary multiplication operation is used to analyze the computational complexity of the algorithms. The proposed algorithm and the 2D-FFT do not use eigenvalue decomposition (EVD) to estimate the range, Doppler information, and angle parameter while the 2D-MUSIC uses the EVD in the multiplication operations. Thus, the complexity analysis of the 2D-MUSIC, the 2D-FFT, and the proposed algorithm is explained using (29) to (31) in Fig. 4, where R denotes the number of spectrum samples of the MUSIC algorithm. As explained in (29), the proposed algorithm is composed of the spectrum partitioning, the extrapolation, and the RELAX based on the FFT. The proposed structure in (29) has a complexity of the number of samples K and K_{E} of the antenna array while the complexity of the 2D-MUSIC is in terms of K^3 in (30). In (30), each component originates from the computation of a sample covariance matrix, its EVD, and the parameter search. For the 2D-FFT in (31), because of the complexity of the number of samples K, it has a considerably lower complexity than the proposed algorithm.

$$C_{\mathrm{prop}} = K[N\log_2 N + 2\log_2 K + z + 3p - p^2] + K_{\mathrm{E}}[p + M\log_2 K_{\mathrm{E}}] \quad (29)$$

$$C_{\mathrm{MUSIC}} = N^2K^3 + N^3K^3 + R[N^2(K+1)K(N-1) + N^2] \quad (30)$$

$$C_{\mathrm{FFT}} = KN\log_2 N + NK\log_2 K \quad (31)$$

IV. SIMULATION

This section assesses the estimation performance of the proposed algorithm compared with that of the conventional algorithms, such as FFT and MUSIC, through various simulations.

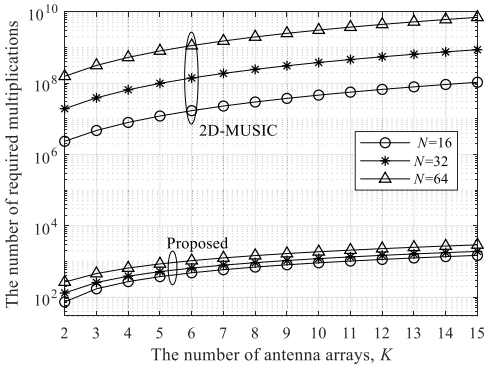

FIGURE 4. Complexity analysis results.

A. SIMULATION ENVIRONMENT

To verify the estimation performance of the proposed algorithm, two simulations are considered. In the first simulation, the spectra of the proposed algorithm, FFT, and MUSIC for DOA are obtained. In the other simulation, the root mean square error (RMSE) of the three algorithms based on the angular separation of the two targets is determined. The SNR is defined by $SNR = 10\log_{10}\left(\sigma_s^2/\sigma_w^2\right)$ where σ_s^2 denotes the power of the source signal, and σ_w^2 is the noise power. The FMCW radar simulation parameters are listed in Table 1. The two targets are located at 3.0 m from the radar. The RMSE according to the parameters of each algorithm at various SNR is calculated C times for the received signals. The RMSE is defined by $\sqrt{1/c\sum_{n=1}^{C}(\hat{\theta}_n - \theta)^2}$, where C is the number of simulations and set to 10^3, and $\hat{\theta}_n$ is the angle of the target in the n-th Monte-Carlo trial.

TABLE 1. Simulation Parameters

Parameter	Value
Center frequency	24 GHz
Bandwidth	1 GHz
Chirp duration (T)	400 μs
Number of samples per chirp (N)	2,000
Number of chirp per one frame (L)	256

B. SIMULATION RESULTS

When two targets are located at the same distance and different angle from the radar, they cannot be distinguished in terms of angle by the conventional FFT and MUSIC algorithms in case of close spacing between targets. The results of the proposed scheme show that the two targets are distinguished on the angle axis. The DOA resolution is about 13.5° [20]. The performance is compared in terms of the spectral results of FFT, MUSIC, and the proposed algorithm. The SNR was set to 20 dB. Fig. 5 shows the simulation environment of the two targets.

As shown in Fig. 6, each algorithm's output is compared according to the angle interval at $K = 8$. The amplitudes a_1 and a_2 of the two targets are set as 0.9 and 1, respectively. In the simulation results for FFT, MUSIC, and the proposed algorithm, as shown in Fig. 6 (a), two signal peaks are

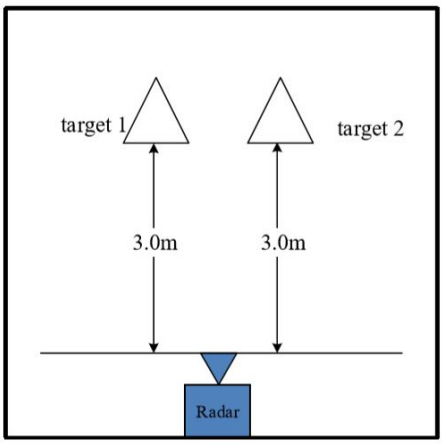

FIGURE 5. Simulation environment of the two targets.

obtained in the angle axis compared with the reference data. This result indicates that, when the two targets are located at $\theta_1 = 20°$ and $\theta_2 = 40°$, respectively, FFT, MUSIC, and the proposed algorithm can distinguish them properly. When the two targets are very close to each other at $\theta_1 = 20°$ and $\theta_2 = 30°$, the FFT simulation result in Fig. 6 (b) shows only a signal peak in the angle axis while the proposed algorithm and MUSIC can still achieve two peaks for the two targets, compared with the reference data. In Fig. 6 (c) with $\theta_1 = 20°$ and $\theta_2 = 26°$, which is less than the angular resolution for $K = 8$, only the proposed algorithm can obtain two peaks for the two targets, compared with the reference data, while the conventional algorithms cannot separate the targets properly. These results indicate that, for small angle separation between the two targets, FFT and MUSIC cannot operate properly while the proposed algorithm can still separate the two targets. Therefore, based on the simulation results, the proposed algorithm can be considered as a high-resolution algorithm.

Fig. 7 shows a comparison between the RMSEs of the proposed and the conventional algorithms versus SNR for different angular separations, with $K = 8$. We will focus on the estimation performance for the first target in the presence of the second target. The angular separations are set at 20°, 10°, and 6°, respectively, as shown in Fig. 6. In Fig. 7 (a), with a wide angular separation of 20°, the RMSEs of both the proposed and the conventional schemes remain low over SNR $= -13$dB. When the angle between the two targets is 10°, i.e., closer to the resolution limitation, as in Fig. 7 (b), the proposed and the MUSIC algorithm yield better results than the FFT algorithm. However, the MUSIC algorithm produces low RMSE only over SNR $= 5$dB. In Fig. 7 (c), where the angular separation is 6°, only the proposed algorithm has a low RMSE and the other algorithms have a poor RMSE performance. Based on these results, we infer that the proposed algorithm has better estimation performance than conventional algorithms such as FFT and MUSIC. The estimation performance of the FFT and MUSIC algorithms deteriorates as the angular separation becomes smaller while that of the proposed algorithm is maintained.

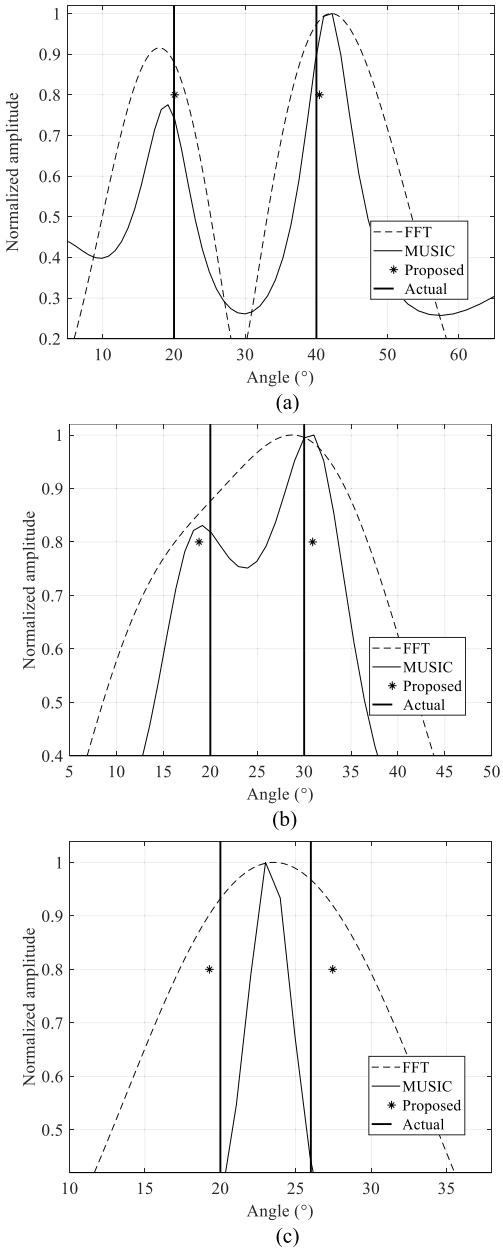

FIGURE 6. Simulation results for different angular separations of the two targets: (a) 20° (b) 10° (c) 6°.

V. EXPERIMENTS

This section presents experiment results to further assess the enhanced performance of the proposed algorithm over conventional ones. An experiment was conducted in an indoor experimental laboratory in South Korea. The overall experimental environment is the same as that described in the Simulation section.

A. EXPERIMENTAL SETUP

We used the 24 GHz FMCW radar system as shown in [20]. Fig. 8 (a) shows a block diagram of the RF front-end module (FEM). Fig. 8 (b) shows various views of the RF FEM. As shown in Fig. 8 (a) and 8 (b), the RF FEM is composed

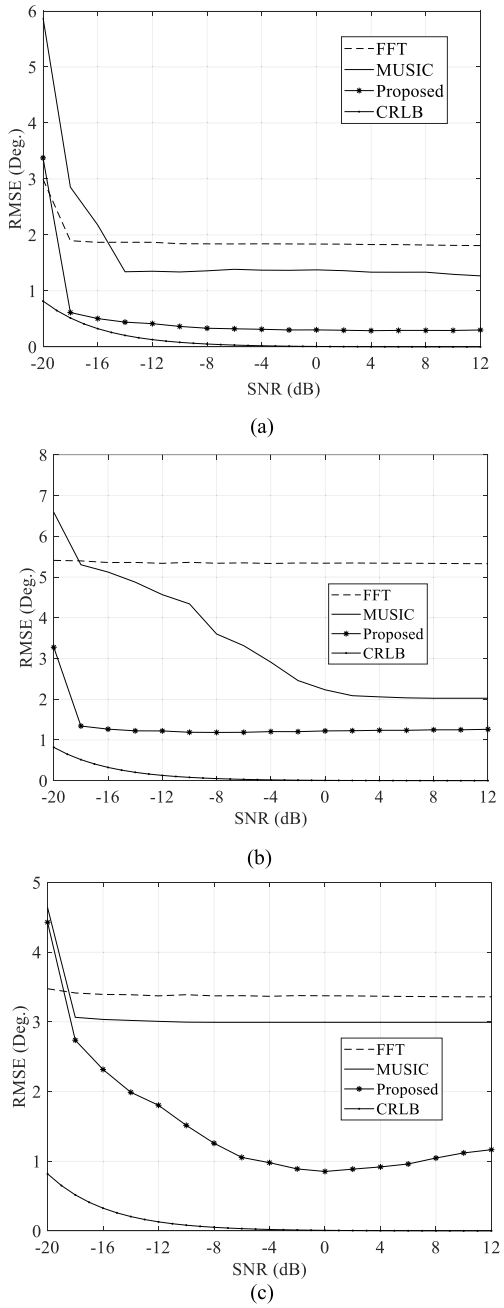

FIGURE 7. RMSEs versus SNR for different angular separations of the two targets: (a) 20° (b) 10° (c) 6°.

of two TX antennas and eight RX antennas. The TX part includes a frequency synthesizer with phase-locked loop (PLL) and voltage-controlled oscillator (VCO). The VCO output is finally connected to the two TX antennas through the power amplifier. In this system, it is not necessary to use the two TX antennas simultaneously. We choose TX antenna 1 with beam-width 26° because, as shown in the next subsection, the azimuth angle to be measured is more than 25°. The RX part consists of low noise amplifiers (LNAs), high pass filters (HPFs), a variable gain amplifier (VGA), and low pass filters (LPFs). The reflected signal passing

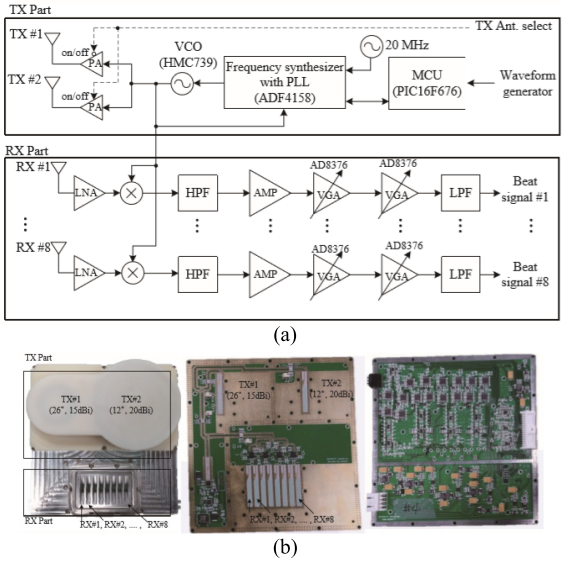

FIGURE 8. FEM architecture [20].

through the LNAs are multiplied with TX signals and then pass the HPFs with a band pass frequency of 150 KHz. The purpose of the HPF is to remove the DC-offset component by the direct conversion architecture of the FMCW radar system [20]. Following HPFs, the eight channels beat signals are passed through the LPFs with a band pass frequency of 1.7 MHz. The noise figure of RX is 8.01 dB and the RX antenna gain is 10 dB. The RX antenna azimuth beamwidth is 99.6° and the elevation beamwidth is 9.9°.

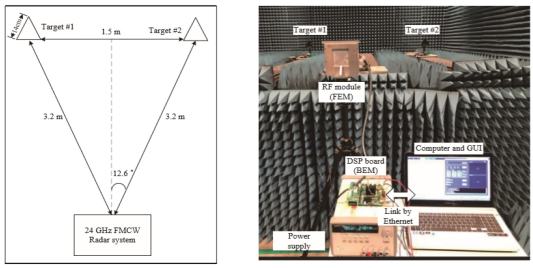

FIGURE 9. Environment and real image of experiment [20].

Fig. 9 shows the experiment environment and a real image in the experiment chamber. As shown in Fig. 9, two targets are located at the same distance from the radar. The experiment was performed inside an anechoic chamber, located at DGIST in Korea. The number of chirps per one frame is set to 256, as shown in Table 2. In the next step, 2048 point FFT was performed for range estimation.

B. EXPERIMENT RESULTS

This subsection presents experiment results to verify the performance improvement of the proposed algorithm. Fig. 10 shows the DOA of target among the range estimation results from channel 1 to channel 6 using 2048 point FFT. In this experiment, speed estimation is not included

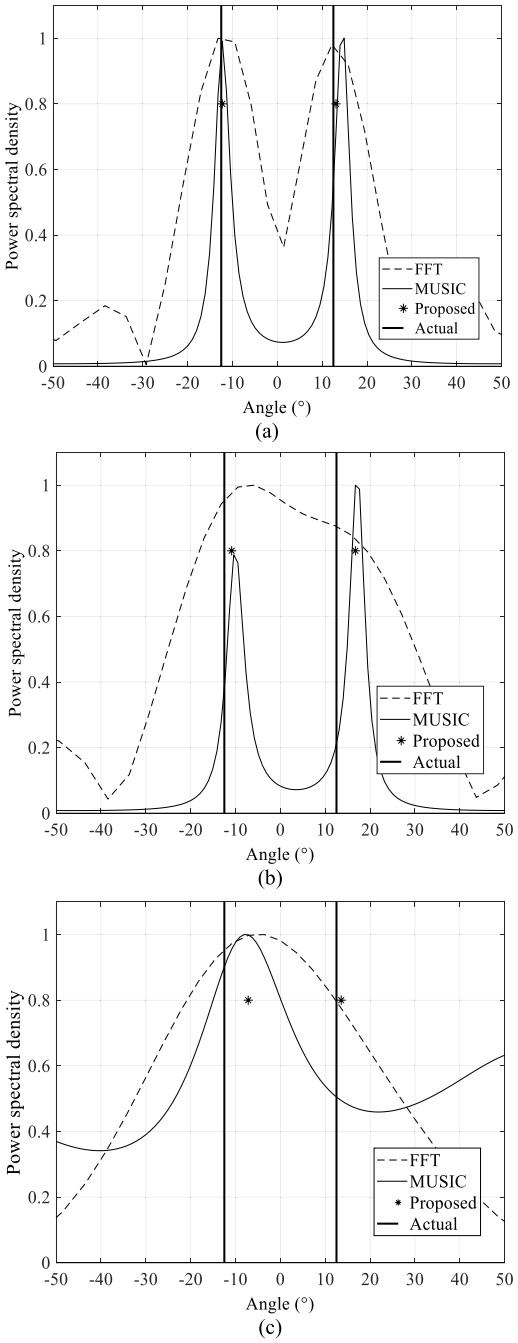

FIGURE 10. Experiment results of DOA for $K = 4$, 6, and 8.

because the two targets are stopped and thus their speeds are zero. According to these experiment results, a range of about 3.07 m is estimated by performing DFT in the sample index domain. In order to detect DOA terms, we use only the range bins corresponding to 3.07 m.

Fig. 10 shows the experiment results with $K = 4$, 6, and 8 for the scenario shown in Fig. 9. In Fig. 10 (a), in the case of $K = 4$, it can be seen that the conventional schemes cannot distinguish between the two targets while the proposed scheme can resolve them, even though there are two targets due to the lack of channels. In the case of $K = 6$ and 8 in Fig. 10 (b) and (c), respectively, the conventional and proposed algorithms can distinguish the two targets. These results show that the proposed scheme achieves an improvement in resolution compared to the conventional ones, due to the virtually increased number of channels.

VI. CONCLUSION

In this paper, an extrapolation-RELAX estimator based on SP for DOA estimation of FMCW radar was proposed. The proposed method considerably enhances the DOA estimation when two targets are very closely located, compared with conventional algorithms. As the proposed algorithm is based on SP, extrapolation, and RELAX, it solves the low resolution problem of conventional algorithms such as MUSIC. The proposed algorithm uses both the magnitude and phase characteristics of the spectrum output of extrapolation while other super-resolution algorithms use only pseudo magnitude information. The simulation results show that, when the angular separation between the two targets is 10°, the MUSIC and the proposed algorithm can distinguish the two targets, but the conventional 2D-FFT algorithm cannot. When the angular separation between the two targets is 6°, only the proposed algorithm can resolve the two targets. With regard to RMSE, when the angular separation between the two targets is 20°, the RMSEs of both the proposed and the conventional schemes remain low regardless of the SNR. When the angular separation between the two targets is 10°, i.e., closer to the resolution limitation, the proposed and the MUSIC algorithm produce better results than the FFT algorithm. When the angular separation is 6°, i.e., under the resolution limitation, only the proposed algorithm yields a low RMSE and the other algorithms exhibit a poor RMSE performance. Experimental and complexity analyses showed that the proposed method has considerably lower complexity than the MUSIC algorithm and can identify adjacent targets that cannot be distinguished by the MUSIC algorithm. Therefore, the proposed method is applicable to FMCW radar owing to its high performance for parameter estimation.

ACKNOWLEDGMENT

(Sangdong Kim and Bong-Seok Kim are co-first authors.)

REFERENCES

[1] J. C. Lin, "Noninvasive microwave measurement of respiration," *Proc. IEEE*, vol. 63, no. 10, p. 1530, Oct. 1975.

[2] S. Kim and K.-K. Lee, "Low-complexity joint extrapolation-MUSIC-based 2-D parameter estimator for vital FMCW radar," *IEEE Sensors J.*, vol. 19, no. 6, pp. 2205–2216, Mar. 2019.

[3] S. Kim, D. Oh, and J. Lee, "Joint DFT-ESPRIT estimation for TOA and DOA in vehicle FMCW radars," *IEEE Antennas Wireless Propag. Lett.*, vol. 14, pp. 1710–1713, 2015.

[4] C. Li, Y. Xiao, and J. Lin, "Experiment and spectral analysis of a low-power *Ka*-band heartbeat detector measuring from four sides of a human body," *IEEE Trans. Microw. Theory Techn.*, vol. 54, no. 12, pp. 4464–4471, Dec. 2006.

[5] M. Tan, B. Wang, Z. Wu, J. Wang, and G. Pan, "Weakly supervised metric learning for traffic sign recognition in a LIDAR-equipped vehicle," *IEEE Trans. Intell. Transp. Syst.*, vol. 17, no. 5, pp. 1415–1427, May 2016.

[6] M.-S. Lee, V. Katkovnik, and Y.-H. Kim, "System modeling and signal processing for a switch antenna array radar," *IEEE Trans. Signal Process.*, vol. 52, no. 6, pp. 1513–1523, Jun. 2004.
[7] G. Wang, C. Gu, T. Inoue, and C. Li, "A hybrid FMCW-interferometry radar for indoor precise positioning and versatile life activity monitoring," *IEEE Trans. Microw. Theory Techn.*, vol. 62, no. 11, pp. 2812–2822, Nov. 2014.
[8] L. Ren, Y. S. Koo, H. Wang, Y. Wang, Q. Liu, and A. E. Fathy, "Noncontact multiple heartbeats detection and subject localization using UWB impulse Doppler radar," *IEEE Microw. Wireless Compon. Lett.*, vol. 25, no. 10, pp. 690–692, Oct. 2015.
[9] Y. Wang, Q. Liu, and A. E. Fathy, "CW and pulse–Doppler radar processing based on FPGA for human sensing applications," *IEEE Trans. Geosci. Remote Sens.*, vol. 51, no. 5, pp. 3097–3107, May 2013.
[10] J. Li, L. Liu, Z. Zeng, and F. Liu, "Advanced signal processing for vital sign extraction with applications in UWB radar detection of trapped victims in complex environments," *IEEE J. Sel. Topics Appl. Earth Observ. Remote Sens.*, vol. 7, no. 3, pp. 783–791, Mar. 2014.
[11] Z. Li, W. Li, H. Lv, Y. Zhang, X. Jing, and J. Wang, "A novel method for respiration-like clutter cancellation in life detection by dual-frequency IR-UWB radar," *IEEE Trans. Microw. Theory Techn.*, vol. 61, no. 5, pp. 2086–2092, May 2013.
[12] X. Hu and T. Jin, "Short-range vital signs sensing based on EEMD and CWT using IR-UWB radar," *Sensors*, vol. 16, no. 12, pp. 2025–2042, Nov. 2016.
[13] G. Wang, J.-M. Muñoz-Ferreras, C. Gu, C. Li, and R. Gómez-García, "Application of linear-frequency-modulated continuous-wave (LFMCW) radars for tracking of vital signs," *IEEE Trans. Microw. Theory Techn.*, vol. 62, no. 6, pp. 1387–1399, Jun. 2014.
[14] Z. Peng, J. M. Muñoz-Ferreras, Y. Tang, C. Liu, R. Gómez-García, L. Ran, and C. Li, "A portable FMCW interferometry radar with programmable low-IF architecture for localization, ISAR imaging, and vital sign tracking," *IEEE Trans. Microw. Theory Techn.*, vol. 65, no. 4, pp. 1334–1344, Apr. 2017.
[15] B.-S. Kim, Y. Jin, S. Kim, and J. Lee, "A low-complexity FMCW surveillance radar algorithm using two random beat signals," *Sensors*, vol. 19, no. 3, pp. 608–624, Jan. 2019.
[16] S. Kim and K. K. Lee, "A low complexity based spectrum partitioning—ESPRIT for noncontact vital radar," *Elektronika Elektrotechnika*, vol. 23, no. 2, pp. 54–58, Jan. 2017.
[17] B. W. Choi, E. H. Bae, J. S. Kim, and K. K. Lee, "Improved prewhitening method for linear frequency modulation reverberation using dechirping transformation," *J. Acoust. Soc. Amer.*, vol. 123, no. 3, pp. EL21–EL25, Feb. 2008.
[18] S. L. Marple, *Digital Spectral Analysis: With Applications*. Englewood Cliffs, NJ, USA: Prentice-Hall, 1987.
[19] H. Akaike, "Fitting autoregressive models for prediction," *Ann. Inst. Stat. Math.*, vol. 21, no. 1, pp. 243–247, 1969.
[20] B. Kim, S. Kim, and J. Lee, "A novel DFT-based DOA estimation by a virtual array extension using simple multiplications for FMCW radar," *Sensors*, vol. 18, no. 5, pp. 1560–1576, May 2018.

SANGDONG KIM was born in Seoul, South Korea, in 1981. He received the B.S. degree from Hanyang University, Ansan, in 2004, the M.S. degree from Hanyang University, Seoul, in 2006, and the Ph.D. degree from Kyungpook National University, Daegu, in 2018, all in electronics engineering. From 2015 to 2016, he was a Visiting Scholar with the University of Florida. Since 2006, he has been a Senior Researcher with the Daegu Gyeongbuk Institute of Science and Technology (DGIST). His research interests include super-resolution algorithms, automotive radar, and vital radar.

BONG-SEOK KIM received the B.S. degree in electronics engineering, in 2006, and the M.S. and Ph.D. degrees in information and communications engineering from Yeungnam University, South Korea, in 2009 and 2014, respectively. From 2014 to 2016, he held a postdoctoral position with the Daegu Gyeongbuk Institute of Science and Technology (DGIST), South Korea. Since 2016, he has been with DGIST, as a Senior Research Engineer. His current interests include multi-functional radar systems and radar signal processing.

YOUNGSEOK JIN received the B.S. and M.S. degrees in communication engineering from Daegu University, South Korea, in 2010 and 2012, respectively. Since 2012, he has been with the Daegu Gyeongbuk Institute of Science and Technology (DGIST), South Korea, as a Researcher. His current interests include radar signal processing and implementation in FPGA/DSP.

JONGHUN LEE received the B.S. degree in electronics engineering and the M.S. and Ph.D. degrees in electrical and electronics and computer science from Sungkyunkwan University, South Korea, in 1996, 1998, and 2002, respectively. From 2002 to 2005, he was with Samsung Electronics Company as a Senior Research Engineer. Since 2005, he has been with the Daegu Gyeongbuk Institute of Science and Technology (DGIST), South Korea, as a Principal Research Engineer and an Adjunct Professor. His primary research interests include detection, tracking, recognition for radar (FMCW and UWB radar), radar-based vehicle sensor, and radar signal processing and sensor fusion. He is an IEEE Senior Member.